NANO LETTERS

2007
Vol. 7, No. 10
3116−3121

Dynamically Configurable Biomolecular Nanoarrays

Suxian Huang,* Eric Schopf, and Yong Chen

Department of Mechanical and Aerospace Engineering, California NanoSystems Institute, University of California, Los Angeles, California 90095

Received July 7, 2007; Revised Manuscript Received September 4, 2007

ABSTRACT

Nanoarrays of distinct DNA and protein biomolecules were fabricated by electrochemically controlling their assembly/release from Au nanoelectrodes on a chip. The surface density, ratio, and activity of the biomolecules assembled on each nanoelectrode in the array can be configured quantitatively and temporally by adjusting the electrochemical potential applied on the nanoelectrode. The dynamically configurable biomolecular nanoarray can potentially activate combinatorial interactions with microbiosystems under the control of an electronic circuit for biological and medical applications.

Biomolecular nanoarrays have attracted significant attention because of their potential biological and medical applications,[1] such as high-sensitive diagnostic tests and low-cost high-throughput analysis of a large amount of different biomarkers for genomics and proteomics.[2,3] Biomolecular nanoarrays can also immobilize and recognize various microbiosystems, such as viruses,[4] bacteria,[5] and cells[6] on substrate surfaces. The progresses at this frontier could establish a prospective combinatorial biochemical "nanofactory" with a range of applications such as biochemical sensors, gene expression platform, drug delivery, gene therapy, and cellular signaling. To fabricate the biomolecular nanoarrays, various top-down lithographic and bottom-up self-assembly nanoscale biopatterning techniques have been developed. The top-down lithographic techniques, such as nanografting,[7] dip-pen,[8] electron-beam,[9] nanocontact,[10] and nanoimprint[11] lithography, can flexibly generate well-defined biomolecular nanopatterns; self-assembled nanoscale particles,[12] polymer,[13] and DNA[14] can generate templates to guide the formation of regular biomolecular nanopatterns. In additional to the nanopatterning, electrochemical techniques have been explored to control and modify biomolecules assembled on electrically addressable electrodes. For example, distinct DNA oligonucleotides have been assembled on carbon nanotubes,[15] and biomolecular surface densities and properties on macro- or microscale electrodes have been modified by electrochemical potentials applied on the electrodes.[16−20] Although these techniques can fabricate homogeneous biomolecular patterns with nanoscale sizes,[8−11] the biomolecular nanoarrays are still in their infancy. Achieving a heterogeneous array of distinct biomolecular patterns with nanoscale spacing has remained elusive;[21] moreover, it is hard to temporally modify the types and densities of biomolecules in a nanoarray. To fabricate biomolecular nanoarrays with the structural complexity that can match biological membranes and control combinatorial interactions with microbiosystems dynamically, the major challenges remain not only in spatially patterning distinct biomolecules with nanoscale feature size and spacing, but also temporally configuring the quantities and activities of the biomolecules in the nanoarrays based on preprogrammed information and active feedbacks. In this letter, we report a technique to fabricate heterogeneous biomolecular nanoarrays with distinct DNA oligonucleotides and biotins/streptavidins by electrochemically controlling the assembly/release of the biomolecules from Au nanoelectrodes. The surface densities, ratios, and activities of the biomolecules on each nanoelectrode were modified quantitatively and temporally by adjusting the amplitude and duration of the electrochemical potentials applied on the Au nanoelectrodes.

The sequences of the four distinct single-stranded DNA oligonucleotides (Stanford PAN Biotechnology Facility, Palo Alto, CA) used in our experiment are listed in Table 1. The 5′ end of the DNA was modified with a thiol linker, and the 3′ end was labeled with fluorophore or biotin. As listed in Table 1, the HS−DNA−FAM, HS−DNA−CY3, and HS−DNA−CY3.5 are labeled with distinct fluorophores with excitation/emission peak wavelengths at 488/525 (FAM), 532/595 (CY3), and 594 nm /615 nm (CY3.5), respectively. The biotin in the HS−DNA−Biotin can react with fluorophore-labeled streptavidins, Streptavidin-Alexa Fluor 350 or Streptavidin-Alexa Fluor 546 (Invitrogen Co.) with fluorescent excitation/emission peak wavelengths at 346/442 or 556 nm/573 nm, respectively. The 1 μM DNA solutions were

* Corresponding author. E-mail: huangsuxian@ucla.edu. Ph: (310) 267-4340.

10.1021/nl071643g CCC: $37.00
Published on Web 09/21/2007

Table 1. Sequences of DNA Oligonucleotides

molecular name	sequence
HS−DNA−FAM	5′ HS−$(CH_2)_6$-TAGTCGGAAGCATCGAAGGCTGAT−FAM 3′
HS−DNA−CY3.5	5′ HS−$(CH_2)_6$-TTTTTTTTTTTTTCCCCCCCCCCCC−CY3.5 3′
HS−DNA−CY3	5′ HS−$(CH_2)_6$-TTTTTTTTTTTTTCCCCCCCCCCCC−CY3 3′
HS−DNA18−CY3.5	5′ HS−$(CH_2)_6$-TAGTCGGAAGCATCGAAG−CY3.5 3′
HS−DNA−Biotin	5′ HS−$(CH_2)_6$-TAGTCGGAAGCATCGAAGGCTGAT−biotin 3′

prepared by dissolving the DNA in 1 M potassium phosphate buffer (pH = 6.9). The 1 μM tris(2-chloroethyl) phosphate was added to the DNA solution to disrupt the formation of disulfide bonds between the thiol linkers. Au electrodes were fabricated by depositing a 5 nm thick Ti adhesive layer and a 30 nm thick Au layer on a 100 nm thick SiO_2 layer on a Si chip by electron beam evaporation. Lateral sizes of the Au electrodes were defined by electron beam lithography with a JEOL 5910 scanning electron microscope (SEM) controlled by Nanometer Pattern Generation System (JC Nabity Lithography Systems). The same SEM was also used for imaging of the nanoelectrodes. Prior to the DNA assembly, the surfaces of the Au electrodes on the SiO_2/Si chip were cleaned in a piranha (H_2SO_4/H_2O_2 = 3:1) bath for 5 min followed by a deoinized (DI) water rinse for 1 min. By immersing the cleaned Au electrodes in the aforementioned 1 μM DNA solution for 30 min at room temperature, the thiolated DNA was assembled on the Au surface by the formation of the S−Au bond. After the assembly, the DNA physically adsorbed on the surface was removed by rinsing the chip in a phosphate-buffered saline (PBS) buffer with 0.02% Tween-20 for 1 min.

The assembly process described above can be reversed by applying a negative potential on the Au electrodes. It has been reported that when the negative potential exceeds a critical value, the DNA can be released from the electrode due to the breakdown of the S−Au bond.[16−18] In our experiments, to control the release process accurately, an electrochemical potential was applied via a standard three-electrode electrochemical setup with the Au electrode on the SiO_2/Si chip as a working electrode, an Ag/AgCl wire as a reference electrode, and a Pt wire as a counter electrode. The chip and all the three electrodes located at ~2 mm from each other were immersed in an electrolyte solution (tris 10 mM, pH 7.3). The applied potential was programmed and controlled via an electrochemical potentiostat (Bio-Logic SAS, France). All the electric potentials applied on the Au electrodes referred in this letter are the potentials applied with respect to the Ag/AgCl reference electrode in the three-electrode setup.

We first used the assembly/release process shown schematically in Figure 1a to fabricate a biomolecular nanoarray with four distinct DNA sequences listed in Table 1. The HS−DNA−FAM was assembled on all the Au nanoelectrodes on a SiO_2/Si chip via the aforementioned assembly process (Figure 1a, left). By applying a −1.6 V potential pulse for 2 s selectively on some of the Au nanoelectrodes, the HS−DNA−FAM was completely released from these selected Au nanoelectrodes (Figure 1a, middle). During the releasing process, the HS−DNA−FAM on the rest of the unselected nanoelectrodes remained intact. After the chip surface was thoroughly rinsed in the PBS buffer with 0.02% Tween-20 for 1 min, a distinct DNA sequence, the HS−DNA−CY3, was then assembled on these selected bare Au nanoelectrodes (Figure 1a, right). The assembly/release procedures were repeated until the HS−DNA−FAM, HS−DNA−CY3, HS−DNA−CY3.5, and HS−DNA−Biotin were selectively assembled to different Au nanoelectrodes. The HS−DNA−Biotin then reacted with the fluorophore-labeled streptavidins, Streptavidin-Alexa Fluor 350, by soaking the chip in the solution of the latter in the PBS buffer (0.05 mg/mL, pH 11.2) for 30 min. Fluorescence images of the array of the nanoelectrodes assembled with the four distinct DNA sequences were taken with different filter sets in a fluorescence microscope (Nikon Eclipse E400) and superimposed into a single fluorescence image shown in Figure 1b. The spiral structure of the Au nanoelectrodes with a line width of ~60 nm is shown in an SEM image in Figure 1c. The fluorophores associated with the HS−DNA−FAM, HS−DNA−CY3, HS−DNA−CY3.5, and HS−DNA−Biotin

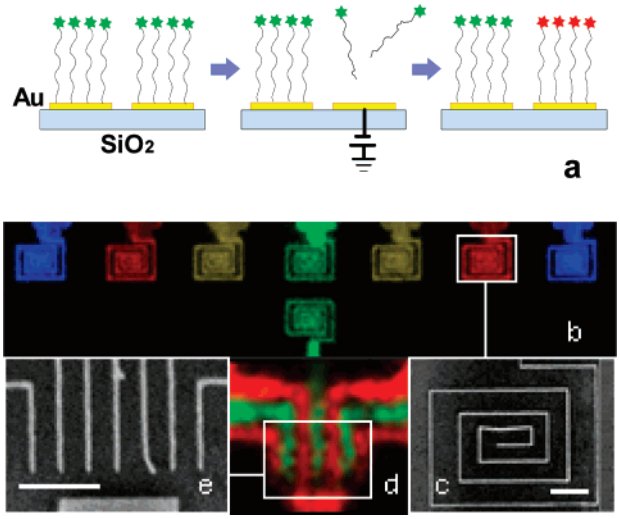

Figure 1. (a) Schematics showing that a DNA sequence is assembled onto Au nanoelectrodes (left), selectively released from one of the nanoelectrodes (middle), and a distinct DNA sequence is reassembled onto the bare Au nanoelectrode (right). (b) A fluorescence image of an array of Au nanoelectrodes assembled with four distinct DNA sequences listed in Table 1 (HS−DNA−FAM, green; HS−DNA−CY3, yellow; HS−DNA−CY3.5, red; and HS−DNA−Biotin−Streptavidin-Alexa Fluor 350 complex, blue.). (c) An (SEM) image showing the spiral structure of the Au nanoelectrodes shown in Figure 1b. (d) A fluorescence image of an array of Au nanoelectrodes assembled with two distinct DNA sequences listed in Table 1 (HS−DNA−FAM, green; and HS−DNA−CY3.5, red). (e) An SEM image showing the structure of the parallel Au nanowire electrodes shown in Figure 1d. Scale bars: 1 μm.

molecules are shown in Figure 1b with green, yellow, red, and blue colors, respectively. As measured with different color filters, the ratio between the average fluorescence intensity from the nanoelectrode with the corresponding DNA to the average intensities from the other nanoelectrodes without the corresponding DNA is approximately >76, and the ratio between the average fluorescence intensity from the Au nanoelectrode with the corresponding DNA to the background intensity from their nearby SiO_2 surfaces is approximately >175. A fluorescence image of a different array of Au nanoelectrodes assembled with two distinct DNA sequences, HS−DNA−FAM (green) and HS−DNA−CY3.5 (red), is shown in Figure 1d, and the structure of the corresponding Au nanoelectrode array with a 65 nm width and a 230 nm spacing between two adjacent electrodes is shown in an SEM image in Figure 1e. The fine structure of the DNA nanopatterns cannot be resolved in the fluorescence image due to the resolution limit of the fluorescence microscope.

The surface densities of the DNA molecules assembled on the nanoelectrodes can also be modified quantitatively by adjusting the amplitude and duration of the potential applied on the Au electrodes as shown schematically in Figure 2a (left and middle). The DNA covalently bonded to the Au surface was gradually released by applying small negative potential pulses on the Au nanoelectrode with amplitudes ranging between $-0.3 \sim -0.9$ V. For example, −0.6 V potential pulses with a duration of 10, 20, 30, and 40 s were applied on different Au nanoelectrodes assembled with the DNA, HS−DNA−CY3.5, and the chip was then rinsed in PBS buffer for 1 min. The average fluorescence intensity of the remaining HS−DNA−CY3.5 covalently bonded to the Au surface was determined, and the relative change of the average fluorescence intensities is shown as the function of the duration of the applied potential pulses in Figure 2b. The amount of the released DNA is linearly proportional to the duration.

Subsequently, negative potential pulses with a constant duration of 10 s and different amplitudes ranged between $-0.3 \sim -0.9$ V were applied on the Au nanoelectrodes assembled with the different DNA sequences listed in Table 1, and the chips were then rinsed in the PBS buffer for 1 min. The relative change of the average fluorescence intensities was measured and is shown as the function of the potential amplitude for the different DNA sequences, respectively, in Figure 2c. The fitting curves of the experimental data shown in Figure 2c indicate that once the potential amplitude exceeds a critical value, the amount of the released DNA increases exponentially as the function of the potential amplitude. The fitting curves for the three 24-mer DNA sequences (HS−DNA−FAM, HS−DNA−CY3, and HS−DNA−CY3.5) coincide with each other within experimental errors, but the fitting curve for the 18-mer DNA sequence (HS−DNA−DNA18−CY3.5) shifts with respect to the other three curves for the 24-mer DNA sequences toward the lower potential magnitude direction, indicating the influence of the DNA structure on the releasing potential.

Composite biomolecules can be assembled on nanoelectrodes with a controllable ratio by the process shown schematically in Figure 2a. After the DNA, HS−DNA−CY3.5, was assembled on an array of four nanoelectrodes (numbered as 1, 2, 3, and 4), they were partially released by applying potential pulses with a fixed amplitude of −0.75 V and a duration of 0, 3, 6, and 9 s on the nanoelectrodes 1, 2, 3, and 4, respectively. A distinct DNA, HS−DNA−FAM, was sequentially assembled onto the bare Au electrode surfaces left by the released HS−DNA−FAM. Fluorescence images of the array are shown in Figure 2d, and the average fluorescence intensities of the HS−DNA−CY3.5 and HS−DNA−FAM on each nanoelectrode are shown in Figure 2e. The amounts of the remaining HS−DNA−CY3.5 decrease and the amounts of the assembled HS−DNA−FAM increase as the linear function of the durations of the potential pulses applied on the nanoelectrodes.

The activities of biomolecules assembled on the Au nanoelectrodes can also be modified by the electrochemical potential applied on the nanoelectrodes as shown schematically in Figure 3a. The biotinylated DNA, HS−DNA−Biotin, was assembled onto the Au nanoelectrodes by soaking the Au electrodes on the SiO_2/Si chip in the 1 μM DNA solution at room temperature for 45 min. To prevent the direct interaction between the streptavidins and Au surface,[22] a short-chain alkanethiol molecule, mercaptohexanol (MCH), was coassembled on the Au surface by soaking the chip in 1 mM MCH in coadsorption buffer (10 mM tris, 50 mM NaCl, pH 7.3) for 30 min. The HS−DNA−Biotin then reacted with the fluorophore-labeled streptavidins, Streptavidin-Alexa Fluor 546, by soaking the chip in the solution of the latter in the PBS buffer (0.05 mg/mL, pH 11.2) for 30 min. During the whole biotin−streptavidin reaction process, a potential with an amplitude of +0.4 V was applied on some of the Au nanoelectrodes selectively to modify the HS−DNA−Biotin activity on the nanoelectrodes. The chip was then rinsed in the PBS buffer for 1 min. A fluorescence image of the HS−DNA−Biotin−Streptavidin-Alexa Fluor 546 complex assembled on an array of Au nanoelectrodes with the potential modulation is shown in Figure 3b. The fluorescence intensities from the nanoelectrodes that were selectively modified by applying the potential during the biotin−streptavidin reaction process are significantly weaker than those from their neighboring nanoelectrodes without applying the potential, indicating that biotin−streptavidin reaction on the Au nanoelectrodes was impeded by the applied positive potential.[23]

The reaction between the biotin and streptavidin can also be quantitatively controlled. Under the same conditions as described above, the HS−DNA−Biotin assembled on the Au nanoelectrodes reacted with the Streptavidin-Alexa Fluor 546 for 48 min. During the biotin−streptavidin reaction, a +0.4 V potential was applied on different Au nanoelectrodes on a chip with a duration of 48, 42, 36, 30, 24, 18, and 0 min, respectively. After rinsing the chip in the PBS buffer for 1 min, the average fluorescence intensity of the HS−DNA−Biotin−Streptavidin-Alexa Fluor 546 complex on each nanoelectrode was measured, and the relative change

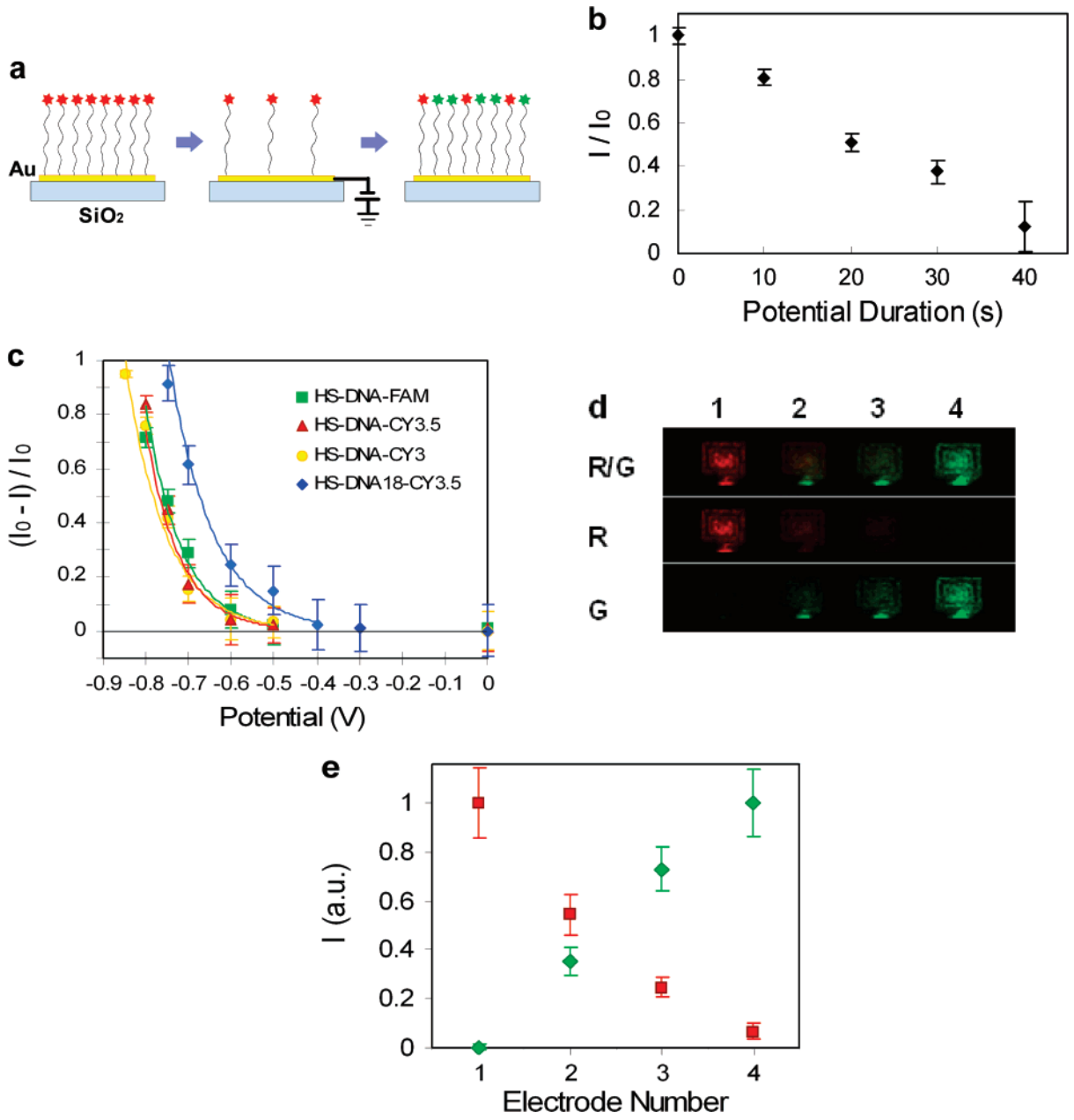

Figure 2. (a) Schematics showing that a DNA sequence is assembled onto an Au nanoelectrode (left), gradually released from the nanoelectrode (middle), and a distinct DNA sequence is then reassembled onto the Au nanoelectrode (right). (b, c) Fluorescence intensity of DNA, assembled on the Au surface changes as the function of (b) the duration and (c) the amplitude of potential applied on the Au electrode. The I_0 and I represent the average fluorescence intensities before and after applying the potential, respectively. The experimental data shown in Figure 2c are fitted with the exponential relation $(I - I_0)/I_0 = \exp[\beta(V - V_0)]$, using β and V_0 as two fitting parameters. From the best-fitting curves, the V_0 can be derived as ~0.4 V for the 24-mer DNA sequences (HS−DNA−FAM, HS−DNA−CY3.5, and HS−DNA−CY3), and ~0.3 V for the 18-mer DNA sequence (HS−DNA18−CY3.5). (d) A superimposed fluorescence image (row R/G) showing two composite DNA sequences, HS−DNA−FAM and HS−DNA−CY3.5, assembled on an array of four Au nanoelectrodes (marked as 1, 2, 3, and 4) with the spiral structure shown in Figure 1c. The filtered fluorescence images (row R and G) showing the fluorescence images of the HS−DNA−CY3.5 and HS−DNA−FAM, respectively. (e) The average fluorescence intensities of the HS−DNA−CY3.5 (red symbols) and HS−DNA−FAM (green symbols) on the nanoelectrodes. The average fluorescence intensities are obtained by collecting more than 1000 data points, and the error bars represent the standard deviation of the fluorescence intensities.

of the fluorescence intensities is shown as the function of the duration of the applied potential in Figure 3c, which indicates that the surface density of the streptavidins on the Au electrode surface decreases linearly as the function of the potential duration.[24]

The modulation of the surface density and activity of the biomolecules on the Au nanoelectrode can be explained quantitatively by the kinetics of the electrochemical reaction. The release of the DNA from the Au electrode is induced by the electrochemical reaction to break the S−Au bond on the Au surface.[16−18] The biotin−streptavidin reaction is modulated by deforming the negatively charged biotinylated DNA under the positive potential applied on the electrode. The experiments show that when a potential with a fixed

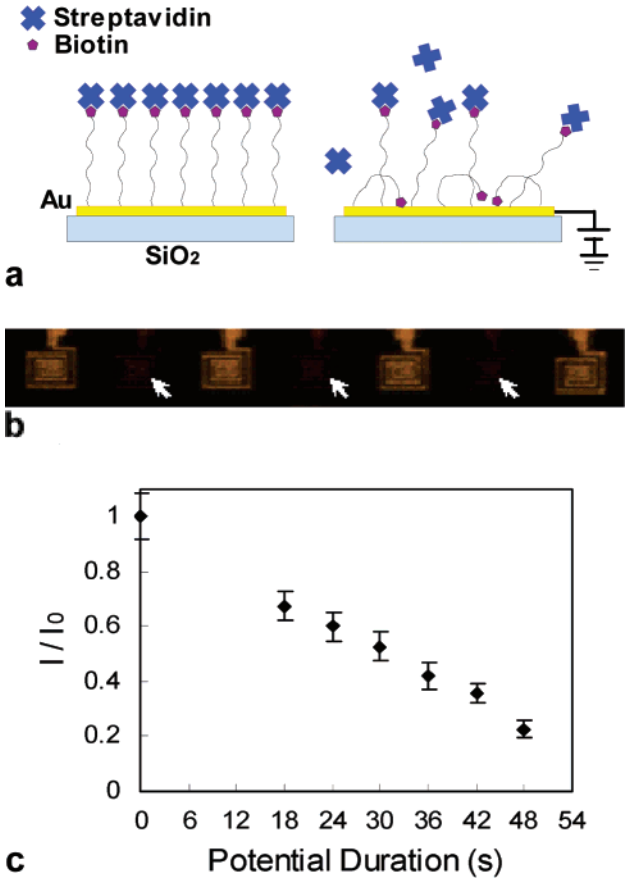

Figure 3. (a) Schematic showing that (left) the biotin ends of the HS−DNA−Biotin assembled on an Au nanoelectrode react with streptavidins; (right) a positive potential is applied on the Au nanoelectrode to attract the HS−DNA−Biotin molecules down to the surface of the nanoelectrode to impede the reaction between the biotins and streptavidins. (b) A fluorescence microscope image of an array of Au nanoelectrodes assembled with HS−DNA−Biotin reacted with Streptavidin-Alexa Fluor 546 with khaki fluorescence color. The nanoelectrodes that were applied with a +0.4 V potential during the biotin−streptavidin reaction are marked by the arrows. (c) The average fluorescence intensity of the HS−DNA−Biotin−Streptavidin-Alexa Fluor 546 complex changes as the function of the duration of the applied potential. The average fluorescence intensities are obtained by collecting more than 1000 data points, and the error bars represent the standard deviation of the fluorescence intensities.

amplitude is applied, the amounts of the DNA released from the nanoelectrodes or the streptavidins conjugated to the nanoelectrodes are approximately linearly proportional to the duration of the applied potential (Figures 2b,e and 3c), which indicates that the reaction rate is a constant under our electrochemical conditions. For zero-order reaction kinetics, $(I(t) - I_0)/I_0 = kt$, where I_0 and $I(t)$ represent the average fluorescence intensities of the biomolecules assembled on the nanoelectrodes before and after applying the potential with a duration of t, respectively, and k is the reaction rate constant. In the electrochemical reaction, $k = k_0 \exp[-\alpha F(V - V_{eq})/RT]$, where V is the potential applied on the electrode, V_{eq} is the equilibration potential, k_0 is the reaction rate constant when $V = V_{eq}$, α is the electronic transfer coefficient, F is the Faraday constant, R is the universal gas constant, and T is the Kelvin temperature. The exponential relationship between k and V has been observed experimentally (as shown in Figure 2c). By fitting the experimental data in Figure 2c, it can be derived that $k_0 = 2.89 \times 10^{-3}$ s^{-1} and $\alpha = \sim 0.25$; $V_{eq} \approx 0.4$ V for 24-mer DNA sequences, and $V_{eq} \approx 0.3$ V for 18-mer DNA sequence. The difference of the V_{eq} might be induced by the difference of the DNA lengths. By adjusting the amplitude and duration of the potential applied on a nanoelectrode, the biomolecules assembled on the nanoelectrode can be configured quantitatively and temporally.

Acknowledgment. We thank Dr. Jeffrey B.-H. Tok, Mr. Yong-Sik Ahn, Mr. Xuejin Wen, and Dr. Zuhua Zhu for their help and discussions. This work was supported by National Science Foundation, through Nanotechnology and Interdisciplinary Research Initiative grant, and by National Institute of Health, through Pacific Southwest Regional Center of Excellence.

References

(1) Stephanopoulos, N.; Solis, E. O. P.; Stephanopoulos, G. *AIChE J.* **2005**, *51* (7), 1858−1869.
(2) Groll, J.; Albrecht, K.; Gasteier, P.; Riethmueller, S.; Ziener, U.; Moeller, M. *ChemBioChem* **2005**, *6* (10), 1782−1787.
(3) Lee, K. B.; Kim, E. Y.; Mirkin, C. A.; Wolinsky, S. M. *Nano Lett.* **2004**, *4* (10), 1869−1872.
(4) Smith, J. C.; Lee, K. B.; Wang, Q.; Finn, M. G.; Johnson, J. E.; Mrksich, M.; Mirkin, C. A. *Nano Lett.* **2003**, *3* (7), 883−886.
(5) Gyorvary, E. S.; O'Riordan, A.; Quinn, A. J.; Redmond, G.; Pum, D.; Sleytr, U. B. *Nano Lett.* **2003**, *3* (3), 315−319.
(6) Gaubert, H. E.; Frey, W. *Nanotechnology* **2007**, *18* (13), 135101.
(7) Wadu-Mesthrige, K.; Xu, S.; Amro, N. A.; Liu, G. Y. *Langmuir* **1999**, *15* (25), 8580−8583.
(8) Lee, K. B.; Park, S. J.; Mirkin, C. A.; Smith, J. C.; Mrksich, M. *Science* **2002**, *295* (5560), 1702−1705.
(9) Hu, W. C.; Sarveswaran, K.; Lieberman, M.; Bernstein, G. H. *IEEE Trans. Nanotech.* **2005**, *4* (3), 312−316.
(10) Li, H. W.; Muir, B. V. O.; Fichet, G.; Huck, W. T. S. *Langmuir* **2003**, *19* (6), 1963−1965.
(11) Falconnet, D.; Pasqui, D.; Park, S.; Eckert, R.; Schift, H.; Gobrecht, J.; Barbucci, R.; Textor, M. *Nano Lett.* **2004**, *4* (10), 1909−1914.
(12) Cai, Y. G.; Ocko, B. M. *Langmuir* **2005**, *21* (20), 9274−9279.
(13) Jung, J. M.; Kwon, K. Y.; Ha, T. H.; Chung, B. H.; Jung, H. T. *Small* **2006**, *2* (8−9), 1010−1015.
(14) Yan, H.; Park, S. H.; Finkelstein, G.; Reif, J. H.; LaBean, T. H. *Science* **2003**, *301* (5641), 1882−1884.
(15) Lee, C. S.; Baker, S. E.; Marcus, M. S.; Yang, W. S.; Eriksson, M. A.; Hamers, R. J. *Nano Lett.* **2004**, *4* (9), 1713−1716.
(16) Mali, P.; Bhattacharjee, N.; Searson, P. C. *Nano Lett.* **2006**, *6* (6), 1250−1253.
(17) Wang, J.; Rivas, G.; Jiang, M. A.; Zhang, X. J. *Langmuir* **1999**, *15* (19), 6541−6545.
(18) Takeishi, S.; Rant, U.; Fujiwara, T.; Buchholz, K.; Usuki, T.; Arinaga, K.; Takemoto, K.; Yamaguchi, Y.; Tornow, M.; Fujita, S.; Abstreiter, G.; Yokoyama, N. *J. Chem. Phys.* **2004**, *120* (12), 5501−5504.
(19) Fan, C. Y.; Kurabayashi, K.; Meyhofer, E. *Nano Lett.* **2006**, *6* (12), 2763−2767.
(20) Mu, L.; Liu, Y.; Cai, S.; Kong, J. *Chem.−Eur. J.* **2007**, *13* (18), 5113−5120.
(21) Lenhert, S.; Sun, P.; Wang, Y. H.; Fuchs, H.; Mirkin, C. A. *Small* **2007**, *3* (1), 71−75.
(22) Herne, T. M.; Tarlov, M. J. *J. Am. Chem. Soc.* **1997**, *119* (38), 8916−8920.
(23) A control experiment was carried out by applying a +0.4 V potential for 30 more min in the PBS buffer (pH 11.2) electrolyte on the nanoelectrodes that had not been applied with the +0.4 V potential previously. After the chip was rinsed again in the PBS buffer (pH 7.4) for 1 min, no change of the fluorescent intensities on those

nanoelectrodes was observed, which confirms that the +0.4 V potential does not change the fluorescent intensities directly, and the change of the fluorescent intensities is due to the modification of the biotin and streptavidin reaction.

(24) A control experiment was also performed with the same aforementioned biotin−streptavidin reaction process without applying the potential, but the biotinylated DNA molecules assembled on the nanoelectrodes were replaced by the nonbiotinylated DNA molecules, the HS−DNA−FAM. The ratio between the average fluorescence intensities of the Streptavidin-Alexa Fluor 546 from the nanoelectrodes assembled with the biotinylated DNA molecules to the ones with the nonbiotinylated DNA molecules is approximately >80, which indicated that the streptavidins nonspecifically bound to the gold surfaces and DNA molecules could be ignored during the modulation of the biotin−streptavidin reaction experiments.

NL071643G